Available online at www.sciencedirect.com

SCIENCE DIRECT®

Tectonophysics 395 (2005) 67–80

TECTONOPHYSICS

www.elsevier.com/locate/tecto

The 1999–2000 seismic experiment of Macas swarm (Ecuador) in relation with rift inversion in Subandean foothills

D. Legrand[a,*], P. Baby[b], F. Bondoux[c], C. Dorbath[c], S. Bès de Berc[d,1], M. Rivadeneira[e]

[a]*IFEA: Institut Français d'Etudes Andines, Whymper 442 y Coruña, Quito, Ecuador*
[b]*IRD (UR154), Casilla 12-1209, Lima 18, Peru*
[c]*IRD (UR154)-LMTG, 14 Avenue Edouard Belin, 31400 Toulouse, France*
[d]*IRD (UR154)-LMTG, 14 Avenue Edouard Belin, 31400 Toulouse, France*
[e]*Petroproducción, Casilla Postal 17-10-7019, Quito, Ecuador*

Received 17 July 2003; accepted 6 September 2004
Available online 22 October 2004

Abstract

We propose to explain the origin of the double trend in seismicity of the Macas swarm in the Subandean Cordillera of Cutucú (Ecuador) and characterize the corresponding active deformation of that region. For that purpose, seismological and geological data have been used, with the deployment of a temporary seismological array, with geological field observations and image processing. We found that some earthquakes are aligned on a well known NNE–SSW trend corresponding to the orientation of the nodal planes of the reverse focal mechanism of the M_w=7.0 1995 Macas earthquake as for its aftershocks. Nevertheless, many smaller events are aligned on an unexpected NNW–SSE trend inside the Cutucú Cordillera. We interpret these two orientations of the Macas swarm as linked to Subandean basement thrusts inherited from the inversion tectonics of a NNE–SSW trending Triassic–Jurassic rift, which has been uplifted and partly extruded in the Cutucú Cordillera. The present partitioning of this part of the Subandean deformation is controlled by pre-existing NNE–SSW to NNW–SSE Triassic–Jurassic normal faults that have been subsequently compressed–transpressed and reactivated into reverse faults. Major boundary faults of the rift were NNE–SSW oriented and correspond now to some main Subandean thrusts as confirms the focal mechanism of the 1995 main shock located on the eastern border (Morona frontal thrust) and the orientation of its aftershocks. In the Cutucú Cordillera, the double orientation of present swarm can be interpreted as the result of accommodation of deformation along NNW–SSE pre-existing faults inside the inverted rift system, linked to the motion of the Morona frontal NNE–SSW thrust.

Keywords: Ecuador; Inversion tectonics; Seismic swarm; Subandean foothills

* Corresponding author. University of Chile, Departamento de Geofísica, Blanco Encalada 2002, Santiago, Chile. Fax: +56 2 696 8686.
E-mail addresses: denis@dgf.uchile.cl (D. Legrand), Patrice.Baby@ird.fr (P. Baby), mrivadeneira54@yahoo.com.mx (M. Rivadeneira).
[1] Now at BRGM Guadeloupe, Villa d'Huy, Morne Notre Dame, 97139, France.

0040-1951/$ - see front matter
doi:10.1016/j.tecto.2004.09.008

1. Introduction

The purpose of this study is to characterize the active deformation of the Cordillera of Cutucú to explain the origin of the double trend in seismicity of the Macas swarm present. A double approach has been considered: a seismological one by the deployment of a temporary seismic network and a geological one with direct field observations and by processing and interpreting images to reveal fault orientation and focal mechanism.

Numerous geological studies have been carried out in the Subandean foothills and Amazonian lowland of Ecuador known as Oriente basin (Tschopp, 1953; Canfield et al., 1982; Dashwood and Abbots, 1990; Baby et al., 1999; Christophoul et al., 2002a,b), but poor detailed structural analysis have been done in the Subandean Cordillera of Cutucú, whose strong tectonic activity is demonstrated by the Macas seismic swarm and the deformation of recent morphologic markers (Bès de Berc, 2003).

Some seismological studies have also been realized in that region (Yepes et al., 1996) but no geological interpretations have been realized, especially to explain the double trend of the Macas swarm. A M_w=7.0 earthquake occurred the 3rd October 1995 at 23.6 km depth (Engdahl et al., 1998), near the city of Macas, in the southern Subandean foothills of Ecuador (Cordillera of Cutucú). The largest aftershocks determined by Harvard are mainly aligned on a NNE–SSW trend in agreement with the focal mechanism of the main shock. Nevertheless, many small events located with the Ecuadorian network were unexpectedly aligned on a NNW–SSE trend (Yepes et al., 1996). As the Ecuadorian network is mainly in a NW direction with respect to the Macas swarm, the location of these small events could have been affected by the seismological regional station distribution. In order to confirm this orientation and interpret it geologically, a locate network of 10 portative stations has been installed between November 1999 and June 2000 around Macas swarm.

2. Geodynamic setting

Ecuador is situated at the hinge between the SSE–NNW oriented Central Andes and the SSW–NNE Northern Andes (see Fig. 1). This elbow-like position corresponds also to a zone of transition on the subducting Nazca plate, which evolves from flat-slab subduction in southern Peru to 30–40° dipping subduction in Colombia. Furthermore, the Ecuadorian margin is affected by the Carnegie Ridge collision, whose effects have been recently discussed (Gutscher et al., 1999a; Guillier et al., 2001; Bourdon et al., 2003). Hence, this part of the Andes is submitted to high stress changing and, as a consequence, may be responsible of the high volcanic and seismic activity of Ecuador with respect to Peru and Colombia. For example, Ecuador has more than 18 active volcanoes, whereas northern Peru (above 14°S) has no active volcano and Colombia has 14 active volcanoes (Simkin and Siebert, 1994). High volcanoes are located in Ecuador (e.g. Mt. Chimborazo, 6310 m; Mt Cotopaxi, 5897 m; Mt Cayambe, 5790 m) and large earthquakes (e.g. the 31/01/1906 M_w=8.8, the 12/12/1979 M_w=8.1, the 14/05/1942 M_w=7.8, the 19/01/1958 M_w=7.7) occurred on the Pacific coast. One of the peculiarities of the Ecuadorian Andes is the occurrence of a large shallow seismic activity in its Subandean foothills (M_w=7.1 1987 Baeza, M_w=7.0 1995 Macas), characterized also by active volcanoes like the Sumaco and the Reventador (recently reactivated from November 2002).

The Nazca plate is subducting under the South America plate with a rate of 58±2 mm/year at the latitudes of Ecuador (Trenkamp et al., 2002). GPS measurements indicate an approximately due east-oriented motion of the Nazca plate relative to stable South America, which is oblique at the Ecuador trench (Kellog and Vega, 1995; Trenkamp et al., 2002) and generating a mainly E–W compression (Ego et al., 1996; Gutscher et al., 1999a,b). Deformation in the high Ecuadorian Andes has been mainly driven by the dextral Dolores Guayaquil Megashear (DGM) zone (Winter et al., 1993; Deniaud et al., 1999; Trenkamp et al., 2002), which marks the suture zone between the Ecuadorian coastal block of oceanic substratum accreted during Paleogene times at the South American continental margin (Benitez, 1995; Jaillard et al., 1995). East of the DGM, the Ecuadorian Andes consist of an eastward orogenic wedge (Cordillera Oriental and Subandean foothills), where structural pattern is dominated by compressive and transpressive defor-

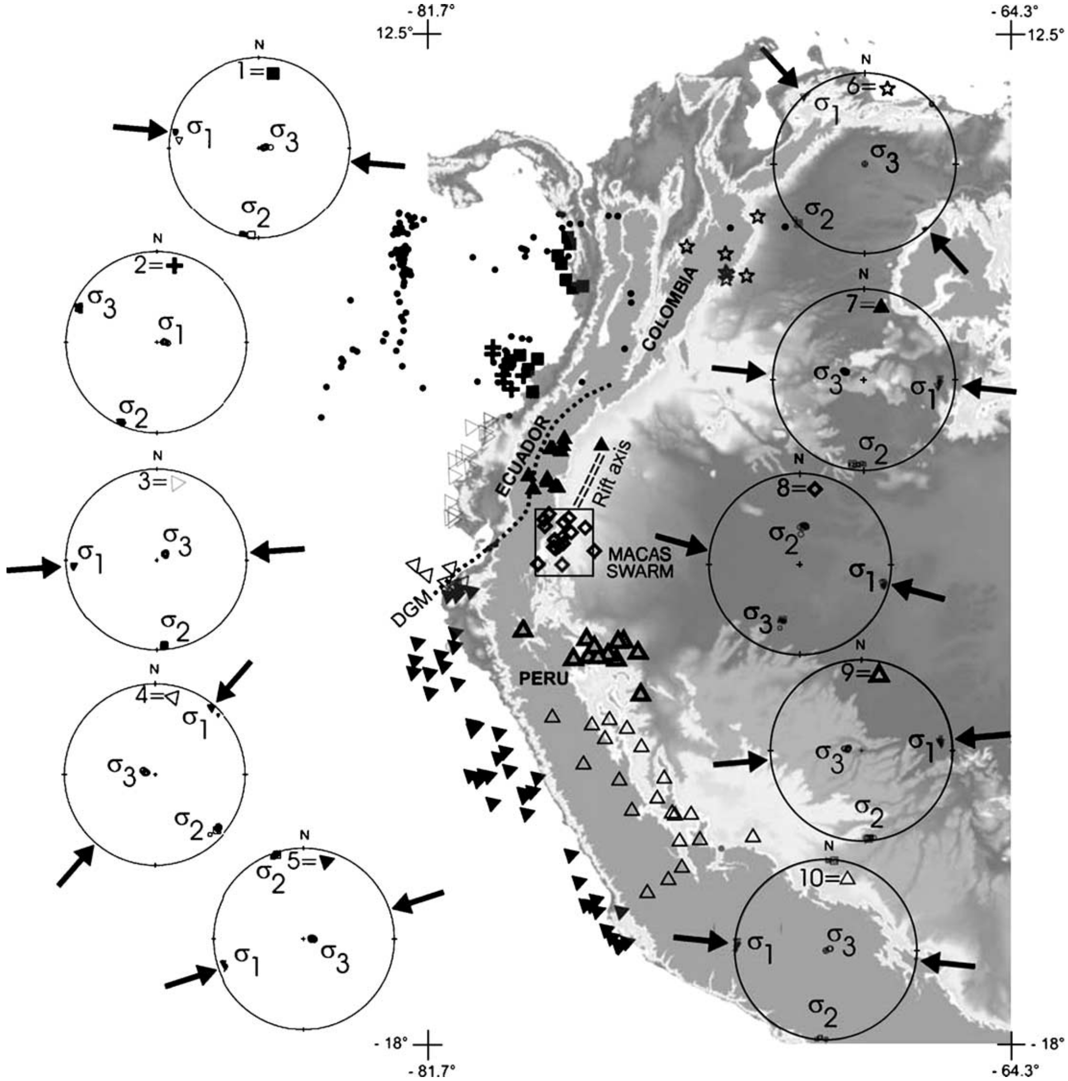

Fig. 1. Elevation map of the north Andean curvature (Gtopo 30 DEM) and shallow (depth<50 km) earthquakes (M_w>5.0) of the Harvard catalog (1977–2000) that have focal mechanism for 10 different regions and the corresponding stress tensors (see also Table 1). Circles correspond to earthquakes that have not been used for stress tensor determinations. For the swarm of Macas, three additional events have been included (10/05/1963, 03/11/1963, 21/06/1967: Chinn and Isacks, 1983; see also Fig. 3). DGM=Dolores Guayaquil Megashear.

mation (Aspden and Litherland, 1992; Baby et al., 1999; Pratt et al., 2002).

3. Present day state of stress

3.1. Theoretical background

Orientation and shape of the stress tensor can be deduced from seismological data. One way is to calculate it from pre-determined focal mechanisms of earthquakes (Angelier and Mechler, 1977; Gephart and Forsyth, 1984; Carey-Gailhardis and Mercier, 1987). Another way is to calculate it at the same time that focal mechanisms, from P wave polarities (Rivera and Cisternas, 1990). In this article, we use the first way. Stress tensors are selected randomly. For each tensor, a 'score' is calculated as the sum of the scalar products between theoretical and observed slip vectors for all mechanisms. A first rough passage selects the N best tensors. These are used as centers for a finer hedge-hog exploration of the space of tensors. The N best solutions (highest 'scores') are finally sorted and shown in Fig. 1, with N=10. The shape factor R of the stress tensor is defined as (Rivera and Cisternas, 1990):

$$R = \frac{\sigma_z - \sigma_x}{\sigma_y - \sigma_x}$$

where σ_x, σ_y and σ_z are the principal stresses (with $\sigma_y>\sigma_x$). σ_z is close to the vertical in order to interpret the shape factor R in a tectonic sense. R varies from -1 to $+1$.

The relationship of the non ordered eigen values σ_x, σ_y and σ_z with respect to the ordered eigen values $\sigma_1>\sigma_2>\sigma_3$ depends on R as follows:

(1) $R<0$ (triaxial compression) $\sigma_y>\sigma_x>\sigma_z$, then $\sigma_y=\sigma_1$, $\sigma_x=\sigma_2$ and $\sigma_z=\sigma_3$
(2) $0<R<1$ (shear) $\sigma_y>\sigma_z>\sigma_x$, then $\sigma_y=\sigma_1$, $\sigma_z=\sigma_2$ and $\sigma_x=\sigma_3$
(3) $1<R$ (triaxial extension) $\sigma_z>\sigma_y>\sigma_x$, then $\sigma_z=\sigma_1$, $\sigma_y=\sigma_2$ and $\sigma_x=\sigma_3$

Focal mechanisms depend on the orientations of the pre-existing faults. In case 1, reverse and strike slip faults are expected. In case 2, we have to consider different cases. If a vertical fault pre-exists, strike slip faults are expected. If one pre-existing fault dip in the y-axis, reverse faults are expected. If the pre-existing fault dip in the x-axis, normal faults are expected. Hence, in this case strike slip, reverse and normal faults may be expected simultaneously. In case 3, only normal and strike slip faults are expected. The particular cases of R=0 corresponds to a uniaxial compression, R=1 to a uniaxial extension, R 1$-$1 to a radial compression and R 1+1 to a radial extension.

As the spatial repartition of events split naturally in different regions (Fig. 1), we assume that the stress tensor is uniform in each region. This hypothesis may not be completely satisfactory, but as far as the number of focal mechanisms available is rather small, there is no way to realize a more precise study.

We use for the inversion all the focal mechanisms for which a focal mechanism exists. Note that events 8, 9, 10, 11 and 12 can be considered as aftershocks of the main shock 7. We can notice that the biggest aftershocks (events 8 and 11) have a similar focal mechanism than the main shock 7. The smallest events (events 9, 10 and 12) have a different focal mechanism and may reflect some local readjustments. We suppose that these local readjustments are representative of the regional stress tensor, are relevant of the local tectonic where local faults have been reactivated by the main shock, explaining why these small events have a different focal mechanism of the main shock. Note that the focal mechanisms of these smallest events are very close to faults compatible with the associated focal mechanism. This diversity of focal mechanism is compatible with the stress tensor we have (case 2 of the above discussion on the stress tensor). Among the focal mechanisms, some have a small double couple component (less than 75%). In order to see the errors inferred by these events, we performed two stress tensor inversions, one with all the data, and another one taking off the events with a double couple part less than 75% (events 7, 8 and 10). We show on Fig. 2 these two stress tensors. The best score with only the best double couples is 0.9471 and with all the data is 0.9411, so the error generated by events with a small double couple component is negligible (less than 0.6%). Looking at the data, the focal mechanisms with a small double couple (events 7, 8 and 10) are very similar to focal mechanism with a higher double component (events 6, 11 and 12, respectively), so that we consider that the double part is well constrained and of small effect on the inversion for the stress tensor. Note that in Fig. 1 and Fig. 1bis, we represent the 10 best solutions, indicating a stable inversion.

3.1.1. Macas region

In order to have a rough idea of stress tensors, we calculate them from CMT Harvard focal mechanisms for shallow (depth<50 km) events of magnitude M_w bigger than 5.0. The whole region has been split into 10 regions for which a unique stress tensor could be calculated (Fig. 1). The general tectonic behavior can be deduced from the shape factor R (Rivera and Cisternas, 1990) of the stress tensor (R<0 for a pure compression, R>1 for a pure extension and 0<R<1 for an intermediate state, Table 1). Few events have not been included because their focal mechanisms were not compatible with the stress tensor of the region (mainly for the coast of Colombia, circles on Fig. 1).

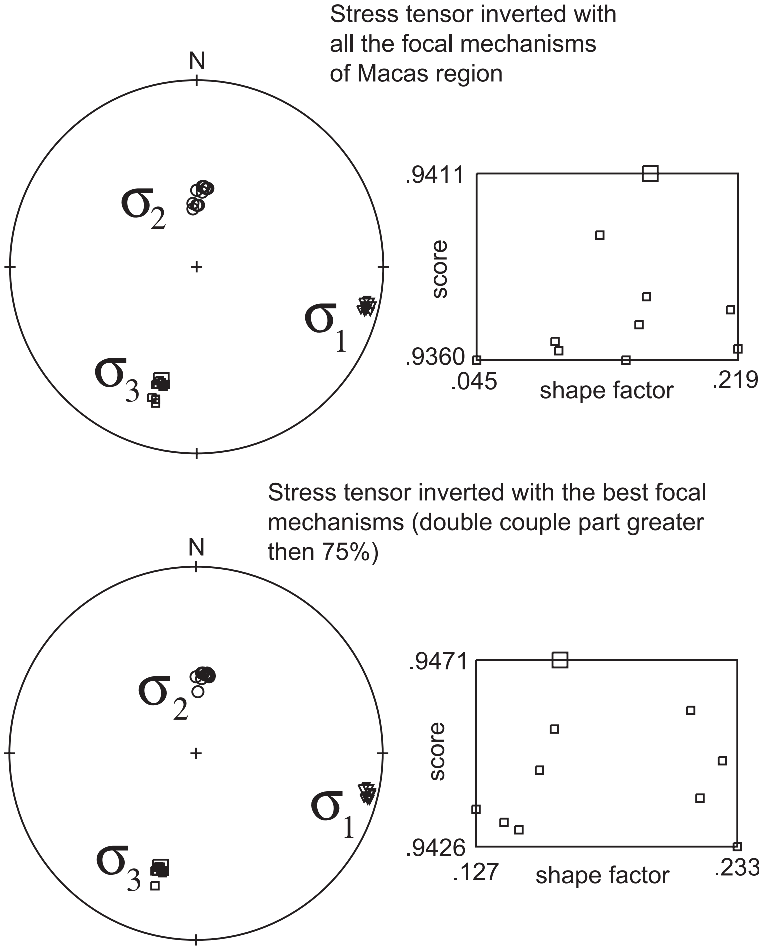

Fig. 2. Determination of the stress tensors from all the focal mechanisms of Macas region (top) and the best focal mechanisms with double-couple component greater then 75% (bottom). As the two stress tensors are very similar, the errors on the stress tensor determination due to non pure double-couple focal mechanisms are negligible.

All the stress tensors are compressional (with a vertical σ_3, Fig. 1, i.e. with R<0, Table 1) except for two regions: the southern part of Colombia Coast (region 2 with crosses in Fig. 1), which is a small extensional region (R>1, Table 1). The second region is the Macas swarm (region 8 with diamonds in Fig. 1), which has an intermediate shear stress tensor (0<R<1, Table 1). This Macas region is a transition zone between two compressional regions (northern Peru and northern Ecuador, Fig. 1, Table 1), characterizing a complex deformation, in an elbow-like position between the change of Peru and Colombia mountain orientation mentioned before. These results are close the one of Ego et al. (1996), and slightly different for the region 6 of Bogotá (stars in Fig. 1) and for the Macas region 8 (diamonds in Fig. 1). For the Macas region, the compressive stress axis σ_1 is roughly in the same direction (N99°E and N104°E). As these are identical, the only difference between the two inversions is the stress regime. It is compressive (σ_3 horizontal) in Ego et al. (1996) and between compressive and transcurrent in this study, for which neither σ_3 nor σ_2 are horizontal and vertical, but have a significant plunge of some 34° and 56°, respectively. These small differences may be attributed to the fact that those authors have not taken into account the 1995 M_w=7.0 Macas earthquake and its aftershocks and the 1995 M_w=6.5 earthquake and its aftershocks

Table 1
Stress tensor characteristics, average of the 10 best solutions

Region	σ_1 strike dip	σ_2 strike dip	σ_3 strike dip	R score
1	280±0.6, 6±0.6	190±0.6, 2.3±0.2	78±1.4, 84±0.6	−1.5±0.1, 0.996±0.0001
2	91±1.7, 83±0.4	204±0.4, 3±0.2	295±0.4, 7±0.4	2±0.1, 0.995±0.002
3	265±0.2, 9±0.3	174±0.2, 5±0.2	54±1.1, 80±0.3	−0.8±0.1, 0.998±0.00002
4	41±0.8, 4±0.2	131±0.9, 9±0.4	285±1.1, 80±0.4	−3±0.4, 0.984±0.0004
5	251±0.5, 8±0.4	341±0.5, 3±0.4	89±2.3, 82±0.4	−0.3±0.1, 0.709±0.0003
6	318±0.3, 0.3±0.1	228±0.3, 0.3±0.1	282±2.4, 90±0.1	−0.33±0.1, 0.973±0.0007
7	93±1, 18±0.4	185±0.9, 6±0.3	294±0.6, 71±0.4	−0.14±0.1, 0.971±0.0004
8	104±0.04, 5±0.5	6±1.0, 56±0.9	198±0.5, 34±0.9	0.17±0.1, 0.944±0.00005
9	84±0.6, 13±0.4	174±0.6, 3±0.2	278±0.9, 77±0.4	−1.84±0.1, 0.991±0.0002
10	274±0.7, 1±0.6	184±0.7, 1±0.3	113±0.3, 89±0.7	−1.39±0.1, 0.845±0.0001

R is the shape factor (see text).

in the Bogotá region (these events occurred after their study).

4. Macas seismic and geological background

A M_w=7.0 shallow (23.6 km depth) earthquake occurred the 03/10/1995 at 2.768°S, 77.818°W (Engdahl et al., 1998, event 7 in Fig. 3) near Macas city, in the Subandean Cutucú Cordillera, which constitutes the eastern foothills of the southern Ecuadorian Andes. Subandean deformation in Ecuador is compressive or transpressive and controlled by deep reaching thrusts or reverse faults (Rivadeneira and Baby, 1999). The Subandean foothills comprise two large basements uplift: the relatively simple Napo antiformal culmination (Levantamiento Napo) in the north, and the complex structure of the Cutucú Cordillera in the south, both separated by the Pastaza Depression where developed a large scale humid tropical alluvial fan (Bès de Berc et al., 2003). The Cutucú Cordillera is intensely deformed by a complex reverse faults system (Fig. 3) related to the transpressive-driven inversion of a NNE–SSW Triassic and Jurassic rift (Baby et al., 1999; Christophoul, 1999; Rivadeneira and Baby, 1999). This inverted rift system disappears to the northeast below the foreland Tertiary deposits of the adjacent Oriente foreland basin as shows seismic profiling of the PETROPRODUCCION oil fields (Fig. 4). Seismic sections along the inverted rift system do not show detachment in the basement and reverse faults root probably in the mantle lithosphere. The core of the Cutucú Cordillera is formed by the Santiago Formation (Fig. 5), which corresponds to the extruded Triassic and Jurassic rift sedimentary fill (Christophoul, 1999). Quaternary geomorphic markers, as alluvial terraces of the Upano valley on the back limb of the Cutucú Cordillera, are deformed by thrust faults (Bès de Berc, 2003). These recent deformations are consistent with the strong seismicity recorded in this zone (Fig. 3).

The largest USGS aftershocks of the 1995 Macas earthquake are located on a NNE–SSW trend (Fig. 3), in agreement with the focal mechanism of the main shock. Nevertheless, many small aftershocks (of local magnitude M_L<4.0) have also been recorded on a NNW–SSE perpendicular trend few days after the main shock (Yepes et al., 1996; Alvarado et al., 1996) and more than 5 years after (Fig. 6, this study). The significance of these two orientations will be discussed latter on.

5. Description of the 1999–2000 seismological field experiments

As seismic activity is high from the 1995 Macas event until present, and in order to confirm the NNW–SSE orientation, a temporary seismological array and structural analysis have been carried out in the Cordillera of Cutucú. Ten stations (eight L4-3D 3 components 1 Hz and two mark product 1 vertical 2 Hz component) have been installed around and inside the Macas swarm between November 1999 and June 2000 (Fig. 6) in order to precise hypocenter locations. Each station was recording time with GPS system. The sample rate of these stations was 50 Hz. Two stations were continuously recording with REFTEK

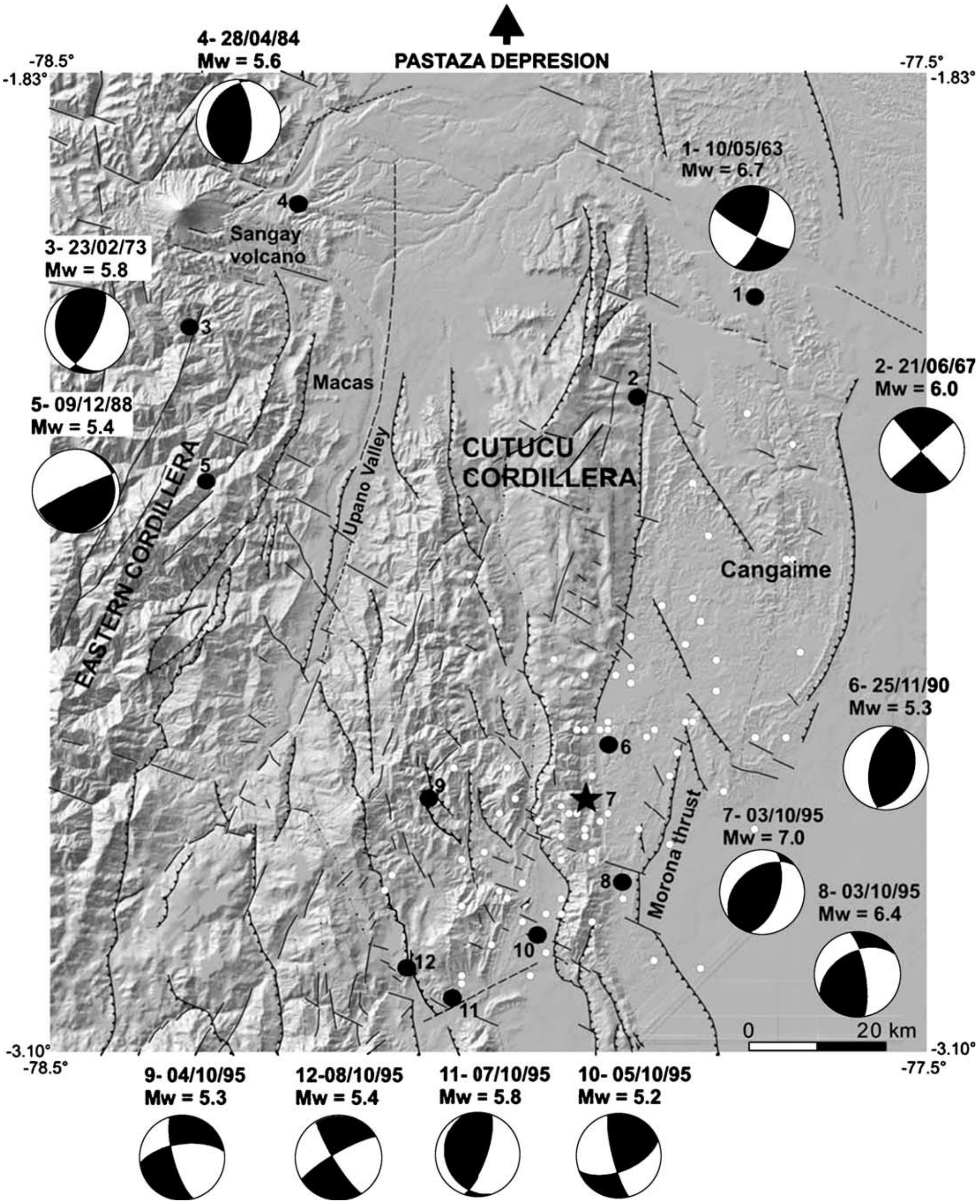

Fig. 3. Focal mechanisms (black points) of shallow (depth<50 km) earthquakes (M_w>5.0) of the Harvard catalog (1977–2000) plotted on the DEM and structural map of the Macas region (Savane software © IRD/MS, France). Three additional events have been included (10/05/1963, 03/11/1963, 21/06/1967: Chinn and Isacks, 1983). The 23.6-km depth 1995 event (number 7, black star) has a focal mechanism compatible with the transpressive Morona frontal thrust. Aftershocks of the 1995 Macas earthquake (white points) are also represented (Harvard catalog, except for the main shock for which we used the more precise Engdahl et al., 1998 determination). Aftershocks are aligned mainly NNE–SSW in agreement with the focal mechanism of the main shock of Macas, 1995.

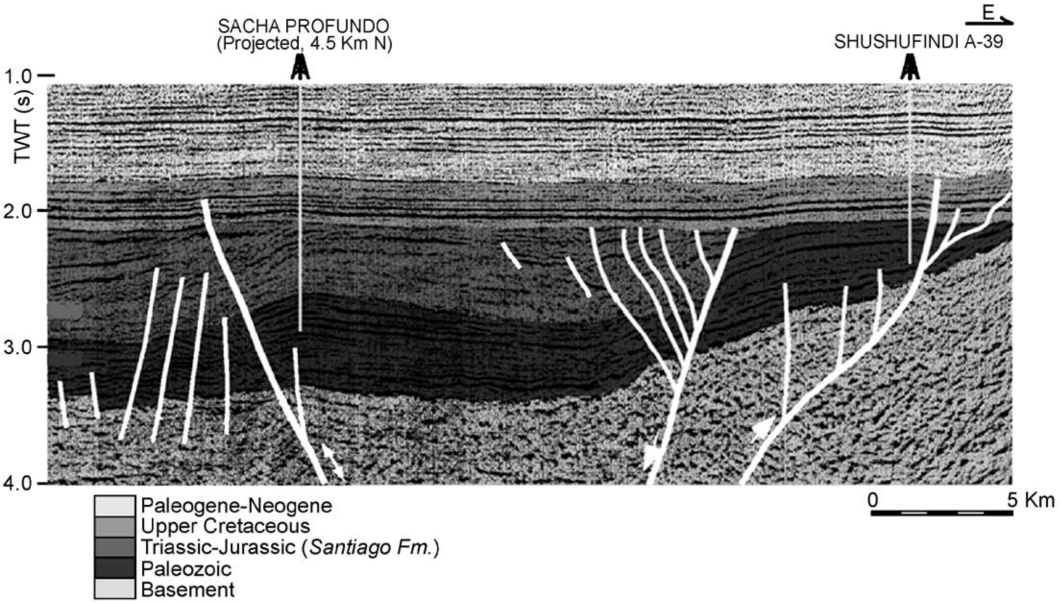

Fig. 4. Seismic reflection section crossing the inverted NNE–SSW Triassic and Jurassic rift of the Oriente basin (modified from Diaz et al., 2003), which merges in the Cutucú Cordillera.

data acquisition system (MIASAL and YAP), because of difficulty access of these stations located in the Amazonian rain forest and that could be reached only with a small plane. The eight other stations were recording with triggering LEAS data acquisition systems. Stations MC6Z and MC7Z were transmitted by telemetry to Cerro Bosco CBOS (Fig. 6).

6. Location of the 1999–2000 events

In a first step, events have been pre-located using hypoellipse code (Lahr, 1995). The model of propagation have been deduced from seismic sections of the Oriente foreland basin (Rivadeneira and Baby, 1999) and compared with a microseismic experiment in the southern Peruvian Ucayali basin used for structure tomography (Mallick and Drummond, 1999). In a second step, relative localizations using the Master Event technique (Spence, 1980; Besse, 1986) have been done (with the a priori information of the hypocenters given by hypoellipse code). In a third step, we performed a joint determination of the velocity structure and the location using the latest version simulps12 (Evans et al., 1994) of the Thurber (1983) method, using as input the travel time data of the events previously located by the master event code. The horizontal error is for 95% of events inferior to 1 km. The error of depth is less than 2 km, except for 20 events for which it is between 2 and 3 km. Most events are between 0 and 25 km depth, and few events are deeper, until 181 km depth, corresponding to the subduction of the Nazca plate. Some events are aligned on the NNE–SSW trend corresponding to the orientation of the nodal planes of the reverse focal mechanism of the M_w=7.0 1995 Macas earthquake, but most of the events are aligned on a NNW–SSE trend inside the Cutucú Cordillera (Fig. 6).

7. Inversion tectonics and seismological data

Hypocenters have been plotted on the geomorphic and structural map of the Cordillera of Cutucú (Fig. 6) obtained from DEM (Savane software, © IRD/MS, France), satellite imagery interpretation, field studies and revised geological maps of PETROPRODUCCION. Our structural map shows two main systems of reverse faults and multi-kilometric folds. The first one has the regional N–S to NNE–SSW orientation and includes the principal bounding thrusts of the Cutucú

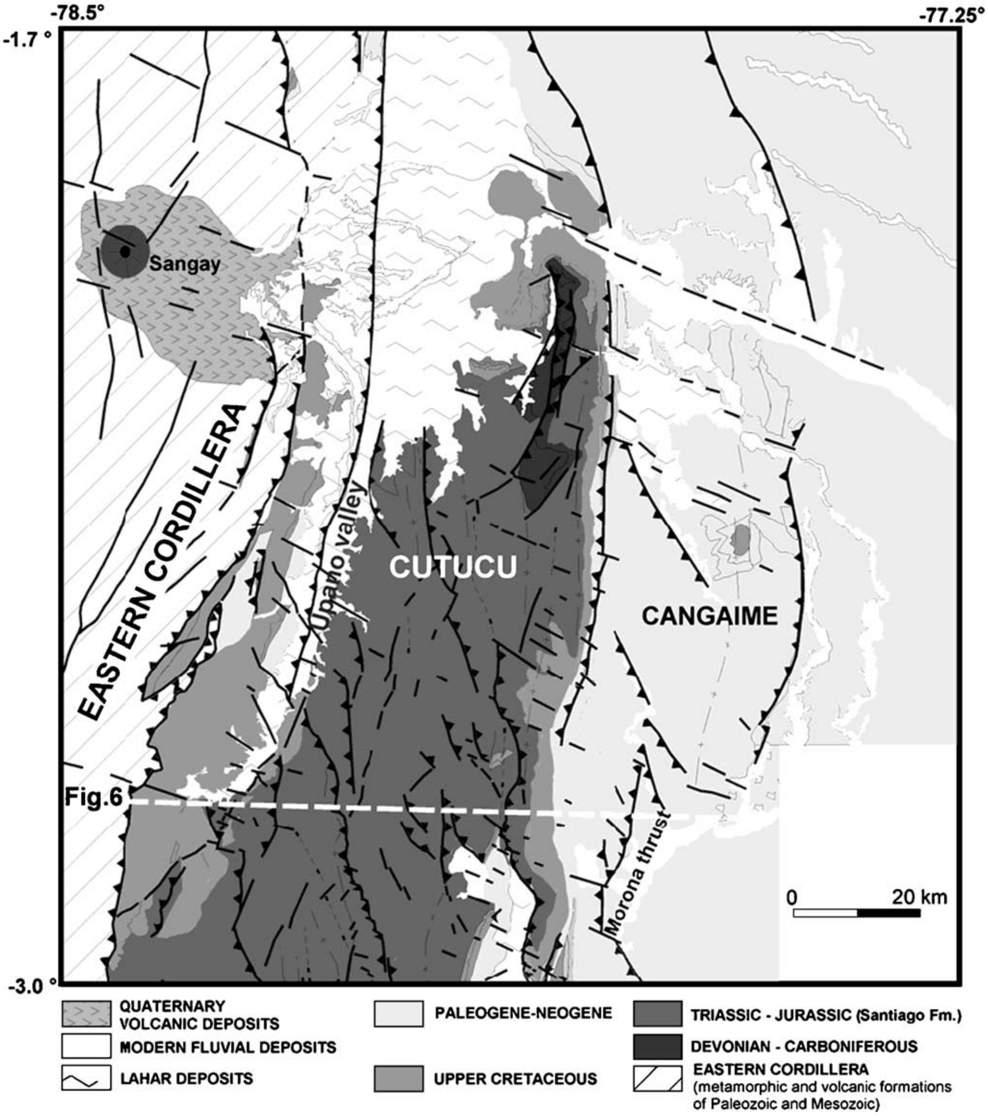

Fig. 5. Geological map of the Macas region.

Cordillera. The 1995 main shock and its aftershocks and a small cluster recorded by our seismic array are located in the frontal limb of the Cutucú Cordillera (Fig. 6). The 1995 main shock (23.6 km depth) probably occurred on the west dipping NNE–SSW reverse fault (Fig. 3), which merges 15 km more to the east (Morona frontal thrust). We will discuss below the origin of this major fault. The second system of reverse faults and folds is oriented NNW–SSE as the main trend of the present Macas seismic swarm confirmed by our experiment.

The cross-section of Fig. 7 has been constructed from surface data and hypocenters plotting obtained from our experiment, inspiring from seismic profiling (Fig. 4) of the northeastern prolongation of the Triassic and Jurassic rift, inverted by transpression and extruded in the Cutucú Cordillera (Christophoul, 1999; Rivadeneira and Baby, 1999). Inverted basins and their associated structures have been recognized on every continent (Lowell, 1995) and rift inversion is common in the Andes (Uliana et al., 1995; Branquet et al., 2002). Earthquake locations show reverse faults

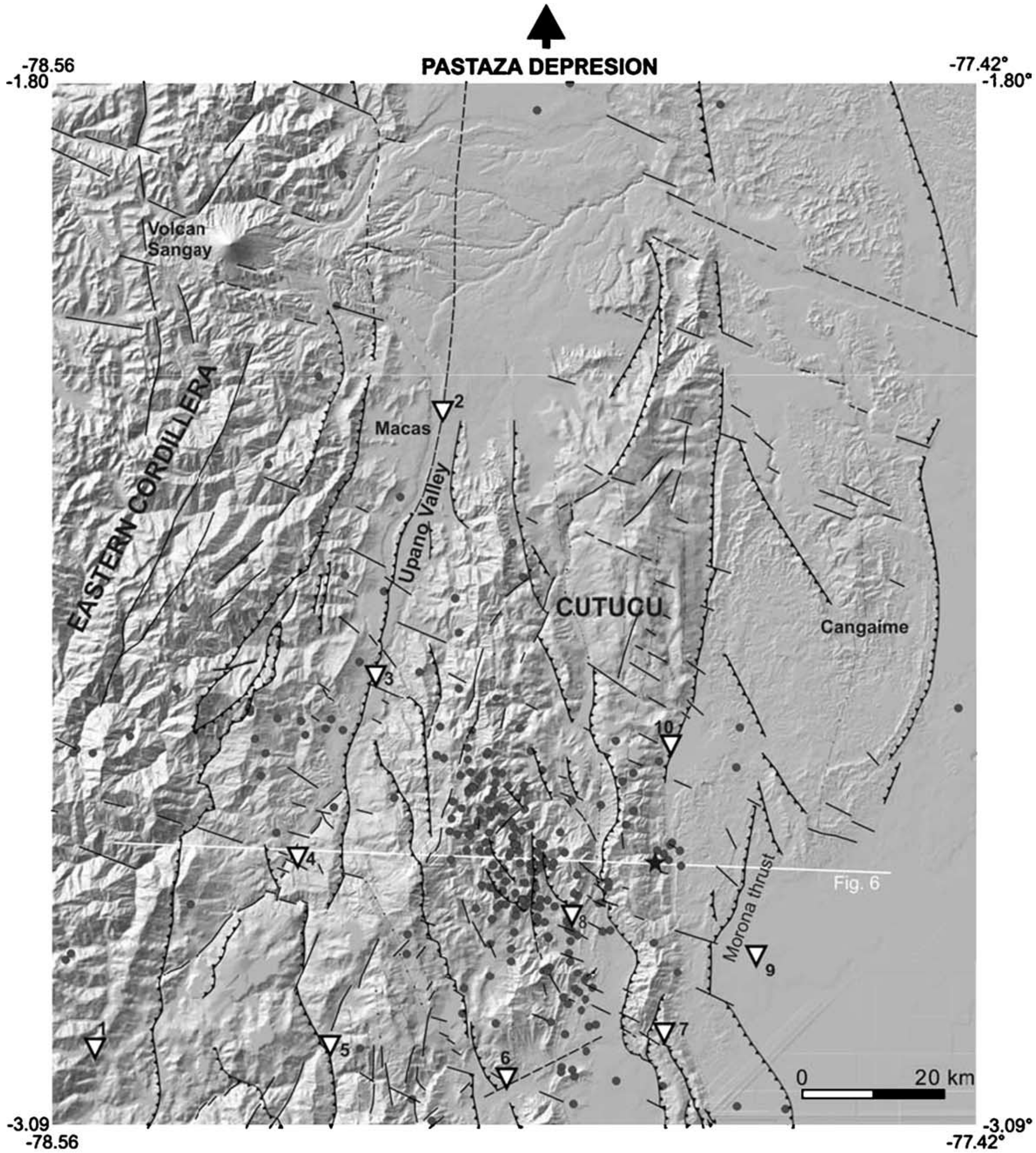

Fig. 6. Seismicity (grey dots) recorded during the 1999–2000 temporary seismic array plotted on the DEM (Savane software © IRD/MS, France) and structural map with locations of the 10 seismic portable stations (yellow triangles: 1: Cerro Bosco, 2: Mac2, 3: Mac3, 4: Mac4, 5: Mac5, 6: Mac6, 7: Mac7, 8: Yaupi, 9: Moróna, 10: Miasal).

(Fig. 7A) in accordance with regional seismic reflection data (Fig. 4). To the east, they limit the Morona frontal thrust where is located the 23.6 depth 1995 main shock. This reverse fault can be interpreted as a major reactivated and inverted normal fault of the eastern border of the Triassic–Jurassic rift (Fig. 7B). Jurassic and Cretaceous volcanic bodies (Christophoul, 1999; Barragán and Baby, 1999), which line

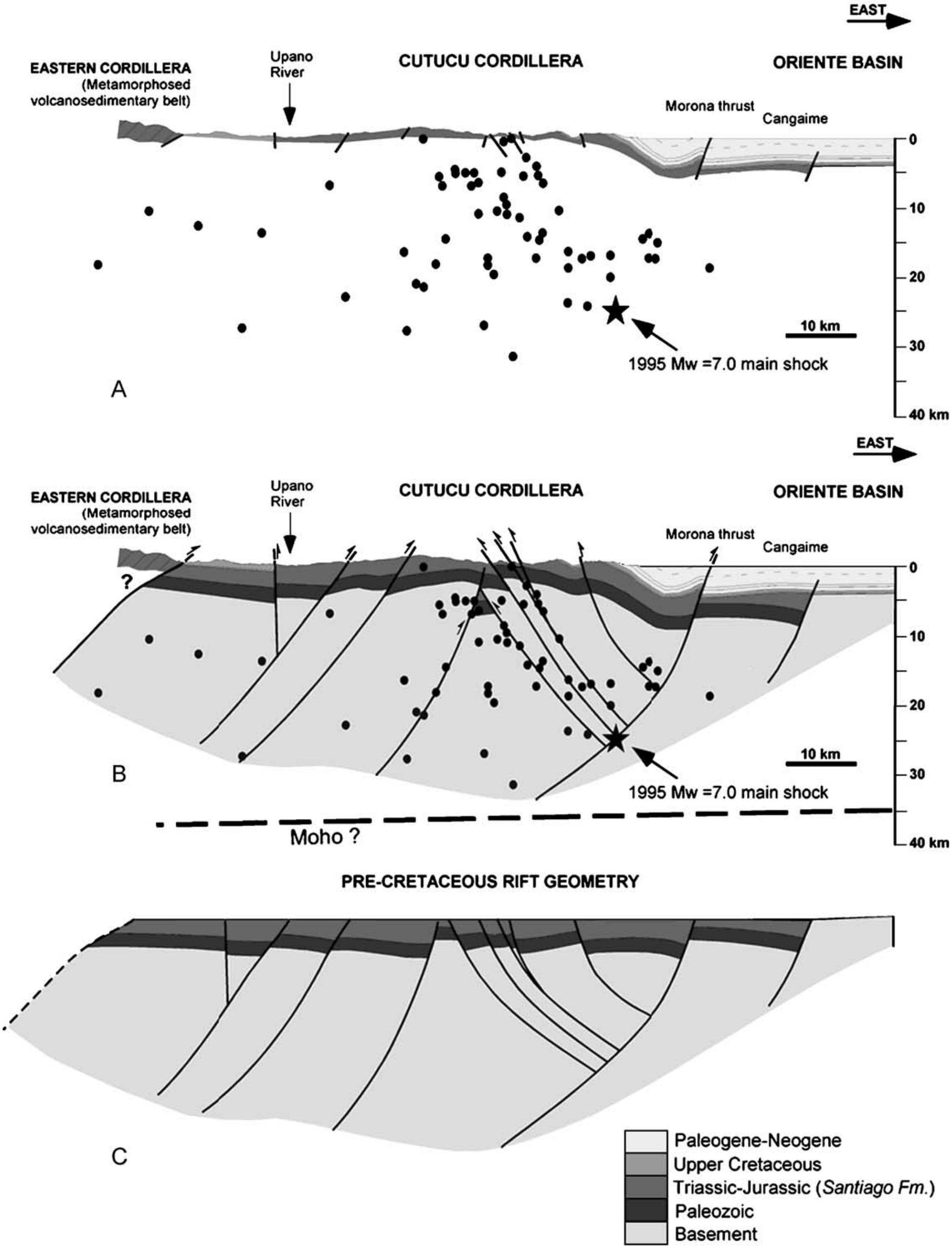

Fig. 7. Structural cross-section perpendicular to the Cutucú Cordillera (location on Figs. 4 and 5): (A) surface data and seismicity recorded during the 1999–2000 temporary seismic array; (B) interpretation of faults geometry inspiring from seismicity and seismic reflection profiling of the northeastern extension of the inverted Triassic–Jurassic rift (Fig. 4); (C) palinspastic restoration showing the pre-Cretaceous rift geometry (pre-inversion state).

the inverted rift, indicate that faults root probably in the mantle lithosphere.

In the core of the Cutucú Cordillera, the NNW–SSE seismic swarm results probably from the reactivation of opposite dip reverse faults, NNW–SSE oriented, that we interpret as inverted bounding normal faults of a basement horst (see palinspastic restoration of the cross-section of Fig. 7C). This interpretation and the NNW–SSE orientation of pre-existing normal faults inside the NNE–SSW trending rift system imply a sinistral transtensional tectonics during Triassic and Jurassic times (Fig. 8). In such a model, the Morona frontal thrust motion (1995 main shock) is accommodated by readjustment of faults within the inverted rift, which induced the NNW–SSE aligned seismicity inside the Cutucú Cordillera.

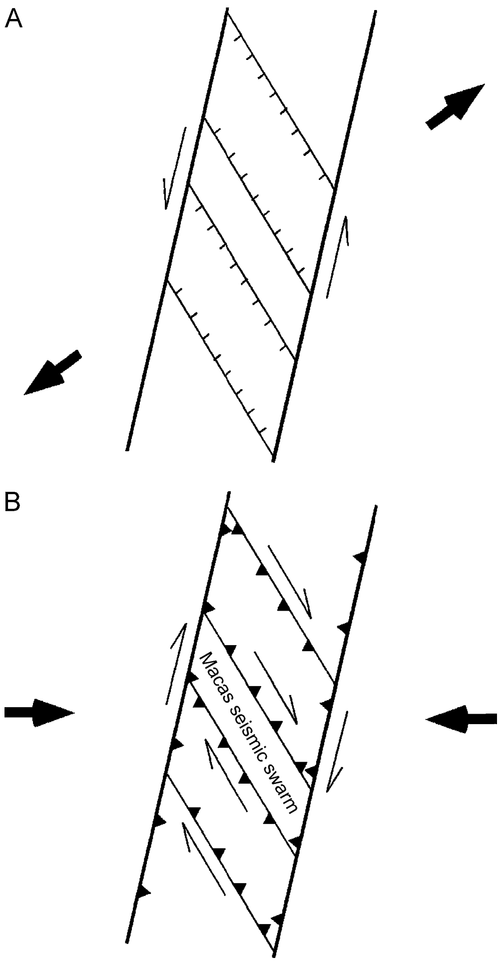

Fig. 8. Structural sketch showing the Triassic–Jurassic rifting phase in transtensive setting (A) and the recent inversion of the rift system with location of the Macas seismic swarm (B).

8. Conclusions

It has been proposed that an inversion tectonics of a NNE–SSW trending Triassic–Jurassic rift penetrates obliquely into the Subandean foothills and merges with the Cutucú uplift. Actual partitioning of this part of the Subandean deformation is controlled by two pre-existing faults orientations of the rift. Original boundary faults of the rift were NNE–SSW oriented and are now reactivated and inverted by compression–transpression as confirms the focal mechanism of the 1995 main shock located on the eastern Morona frontal thrust. Inside the Cutucú Cordillera, the NNW–SSE present swarm can be interpreted as the result of the reactivation of opposite dip reverse NNW–SSE faults inherited from the rift system, which accommodated the initial motion of the eastern Morona frontal thrust (1995 main shock).

South to the Cutucú Cordillera, the rift inversion-related seismicity disappears. This zone corresponds to the Subandean Santiago basin of North-Peru whose deformation is not controlled by pre-existing basement normal faults, but driven by classical thick or thin-skinned thrust tectonics.

Acknowledgements

We thank A. Cisternas for giving us his code for calculating the stress tensor from focal mechanisms and J.C. Ruegg for giving us his Master Event code. We thank IRD for helping us with the seismic station portative network, and PETROPRODUCCION and Fuerzas Armadas del Ecuador for substantial logistic supports. D.L. thanks the French Ministère des Affaires Etrangères and IFEA for a 2-year position in Ecuador. These researches were supported by IRD and INSU grant 99PNSE59.

References

Alvarado, A., Segovia, M., Yepes, H., Guillier, B., Chatelain, J.L., Egred, J., Villagómez, D., Ruiz, M., Samaniego, P., Santacruz, R., 1996. The Mw=6.8 Macas earthquake in the subandean zone of Ecuador, October 3, 1995. Third ISAG, St Malo (France), 17–19/09/1996, pp. 129–132.

Angelier, J., Mechler, P., 1977. Sur une méthode graphique de recherche des contraintes principales également utilisable en tectonique et en séismologie: la méthode des dièdres droits. Bull. Soc. Géol. Fr. XIX (6), 1309–1318.

Aspden, J., Litherland, M., 1992. The geology and Mesozoic history of the Cordillera Real, Ecuador. Tectonophysics 205, 187–204.

Baby, P., Rivadeneira, M., Christophoul, F., Barragan, R., 1999. Style and timing of deformation in the Oriente Basin of Ecuador. 4th International Symposium on Andean Geodynamics (ISAG'99). Univ. Göttingen, Germany, pp. 68–72. Extended Abstracts Volume.

Barragán, R., Baby, P., 1999. A cretaceous hot-spot in the Ecuadorian Oriente Basin: geochimical, geochronological and tectonics indicators. 4th ISAG, Göttingen 4–6/10/99, pp. 77–81. Extended abstracts volume.

Benitez, S., 1995. Evolution géodynamique de la province côtière sud-équatorienne au Crétacé supérieur Tertiaire. Géol. Alp. 71, 5–163.

Bès de Berc, S., 2003. Tectonique de chevauchement, surrection et incision fluviatile (exemple de la zone subandine équatorienne, Haut Bassin Amazonien). Phd thesis, Toulouse III, Paul Sabatier 181 p.

Bès de Berc, S., Soula, J.C., Baby, P., Souris, M., Christophoul, F., Rosero, J., 2003. Geomorphic evidence of active deformation and uplift in a modern continental wedge-topforedeep transition: example of the eastern Ecuadorian Andes. Geophysical Research Abstracts vol. 5, pp. 05941.

Besse, Ph., 1986. Relocalisation relative d'événements sismiques appliqué à la région Sud du lac Ghoubbet situé dans la République de Djibouti. Ph'D, 49 pp.

Bourdon, E., Eissen, J.-P., Gutscher, M.-A., Monzier, M., Hall, M.L., Cotten, J., 2003. Magmatic response to early aseismic ridge subduction: the Ecuadorian margin case (South America). Earth Planet. Sci. Lett. 205, 123–138.

Branquet, Y., Cheilletz, A., Cobbold, P.R., Baby, P., Laumonier, B., Giuliani, G., 2002. Andean deformation and rift inversion, eastern edge of Cordillera Oriental (Guateque-Medina area), Colombia. J. South Am. Earth Sci. 15, 391–407.

Canfield, R., Bonilla, G., Robbins, R.K., 1982. Sacha Oil Field of Ecuadorian Oriente. AAPG Bull. 61, 1076–1090.

Carey-Gailhardis, E., Mercier, J.L., 1987. A numerical method for determining the state of stress using focal mechanisms of earthquake populations: application to Tibetan teleseisms and microseismicity of southern Peru. Earth Planet. Sci. Lett. 82, 165–179.

Christophoul, F., 1999. Discrimination des influences tectoniques et eustatiques dans les basins liés à des zones de convergence: exemples du bassin subandin d'Equateur. Phd thesis, Université Toulouse III, Paul Sabatier, 184 p.

Christophoul, F., Baby, P., Davila, C., 2002. Stratigraphic responses to a major tectonic event in a foreland basin: the Ecuadorian Oriente Basin from Eocene to Oligocene times. Tectonophysics 345 (1–4), 281–298.

Christophoul, F., Baby, P., Soula, J.C., Rosero, M., Burgos, J., 2002. Les ensembles fluviatiles néogènes du basin subandin d'Equateur et implications dynamiques. C. R. Acad. Sci., Paris, Sci. Terre Planètes/Earth Planet. Sci. 334, 1029–1037.

Dashwood, M.F., Abbots, J.L., 1990. Aspects of the Petroleum geology of the Oriente Basin, Ecuador. In: Brooks, J. (Ed.), Classic Petroleum Provinces, Geological Society Special Publication, vol. 50, pp. 89–117.

Deniaud, Y., Baby, P., Basile, C., Ordoñez, M., Montenegro, G., Mascle, G., 1999. Ouverture et évolution tectono-sédimentaire du Golfe de Guayaquil: bassin d'avant-arc néogène et quaternaire du Sud des Andes équatoriennes. C. R. Acad. Sci., Paris 328, 181–187.

Diaz, M., Baby, P., Rivadeneira, M., Christophoul, F., 1999. El Pre-Aptense en la Cuenca Oriente ecuatoriana. Memorias del VIII Simposio Bolivariano—Exploracion Petrolera en las Cuencas Subandinas (Cartagena de Indias, Colombia), vol. 2. pp. 208–222.

Ego, F., Sébrier, M., Lavenu, A., Yepes, H., Egues, A., 1996. Quaternary state of stress in the Northern Andes and the restraining bend model for the Ecuadorian Andes. Tectonophysics 259, 101–116.

Engdahl, E., van der Hilst, R., Buland, R., 1998. Global teleseismic earthquake relocation with improved travel times and procedures for depth determination. Bull. Seismol. Soc. Am. 88, 722–743.

Evans, J.R., Eberhart-Phillips, D., Thurber, C.H., 1994. User's manual for simulps12 for imaging Vp and Vp/Vs: a derivative of the "Thurber" tomographic inversion simul3 for local earthquakes and explosions. Open-File Rep., 94–431.

Gephart, J., Forsyth, D., 1984. An improved method for determining the regional stress tensor using earthquake focal mechanism data: application to the San Fernando earthquake sequence. J. Geophys. Res. 89, 9305–9320.

Guillier, B., Chatelain, J.-L., Jaillard, E., Yepes, H., Poupinet, G., Fels, J.-F., 2001. Seismological evidence on the geometry of the orogenic system in central–northern Ecuador (South America). Geophys. Res. Lett. 28 (19), 3749–3752.

Gutscher, M.A., Malavieille, J., Lallemand, S., Collot, J.Y., 1999a. Tectonic segmentation of the North Andean margin: impact of the Carnegie Ridge collision. Earth Planet. Sci. Lett. 168, 255–270.

Gutscher, M.A., Malavieille, J., Lallemand, S., Collot, J.Y., 1999b. Erratum to "Tectonic segmentation of the North Andean margin: impact of the Carnegie Ridge collision". Earth Planet. Sci. Lett. 170, 155–156.

Jaillard, E., Ordoñez, M., Benitez, S., Berrones, G., Jiminez, N., Montenegro, G., Zambrano, I., 1995. Basin development in an accretionary, oceanic-floored forearc setting: southern coastal Ecuador during late Cretaceous to late Eocene times. In: Tankar, A.J., Suarez, R., Welsink, H.J. (Eds.), Petroleum Basin of South America, Am. Assoc. Pet. Geol. Mem., vol. 62, pp. 615–631.

Kellog, J.N., Vega, V., 1995. Tectonic development of Panama, Costa Rica, and the Colombian Andes: constraints from global positioning system geodetic studies and gravity. In: Mann, P. (Ed.), Geologic and Tectonic Development of the Caribbean plate Boundary in Southern Central America, vol. 295. GSA Special Paper, pp. 75–90.

Lahr, J., 1995. HYPOELLIPSE/Version 3.0: a computer program for determining hypocenter, magnitude and first motion pattern of local earthquake. U.S. Geol. Surv. Open-File Rep. 95 (90 pp).

Lowell, J., 2002. Mechanics of basin inversion from worldwide examples. In: Buchanan, J.G., Buchanan, P.G. (Eds.), Basin Inversion, Geological Society Special Publication, vol. 88. pp. 39–57.

Mallick, B., Drummond, J., 1999. The use of earthquake energy for structure tomography in the northern Ucayali basin. INGEPET 99, III International Seminar, Lima, CD-Rom, 16 p.

Pratt, W., Duque, P., Ponce, M., 2002. Orthogonal deformation in the eastern Andes of Ecuador. 5th International Symposium on Andean Geodynamics (ISAG'02), Univ. Toulouse (France), pp. 485–488. Extended Abstracts Volume.

Rivadeneira, V.M., Baby, P., 1999. La Cuenca Oriente: estilo tectónico, etapas de deformación y caracteristicas geológicas de los principales campos de Petroproducción. PETROECUADOR-IRD edition, Quito, Ecuador, 88 pp.

Rivera, L., Cisternas, A., 1990. Stress tensor and fault plane solutions for a population of earthquakes. Bull. Seismol. Soc. Am. 80, 600–614.

Simkin, T., Siebert, L., 1994. Volcanoes of the World. Geoscience Press, Tucson, Arizona.

Spence, W., 1980. Relative epicenter determination using P-wave arrival-time differences. Bull. Seismol. Soc. Am. 70, 171–183.

Thurber, C.H., 1983. Earthquake locations and three-dimensional crustal structure in the Coyote Lake area, Central California. J. Geophys. Res. 88, 8226–8236.

Trenkamp, R., Kellogg, J.N., Freymueller, J., Mora, H.P., 2002. Wide plate margin deformation, southern Central America and northwestern South America, CASA GPS observations. J. South Am. Sci. 15, 157–171.

Tschopp, H.J., 1953. Oil explorations in the Oriente of Ecuador. AAPG Bull. 37, 2303–2347.

Uliana, A., Arteaga, M., Legarreta, L., Cerdan, G., Peroni, G., 1995. Inversion structures and hydrocarbon occurrence in Argentina. In: Buchanan, J.G., Buchanan, P.G. (Eds.), Basin Inversion, Geological Society Special Publication, vol. 88, pp. 211–233.

Winter, T., Avouac, J.-P., Lavenu, A., 1993. Late Quaternary kinematics of the Pallatanga strike-slip fault (central Ecuador) from topographic measurements of displaced morphological features. Geophys. J. Int. 115 (3), 905–920.

Yepes, H., Chatelain, J.L., Guillier, B., Alvarado, A., Egred, J., Ruiz, M., Segovia, M., 1996. The Mw 6.8 Macas earthquake in the Sub-Andean zone of Ecuador, October 3, 1995. Seismol. Res. Lett. 67, 27–32.